IJSES
International Journal of Scientific Engineering and Science
Volume 9, Issue 1, pp. 110-114, 2025. ISSN (Online): 2456-7361

Corrosion Behavior of Magnesium Alloys for Biomedical Applications

Hossam M. Yehia[1], Omayma A. El-kady[2], Taher Soliman[3], Omnia Mansour[1]
[1]Production Technology Department, Faculty of Technology and Education, Helwan University, Saray-El Qoupa, El Sawah Street, Cairo 11281, Egypt; hossamelkeber@techedu.helwan.edu.eg
[2]Powder Technology Department, Central Metallurgical Research and Development Institute (CMRDI), Helwan 11421, Egypt; o.alkady68@gmail.com
[3]Faculty of Education, Helwan University, Helwan, Egypt.
* Corresponding author: hossamelkeber@techedu.helwan.edu.eg

***Abstract*—** *Magnesium (Mg) is a lightweight metal recognized for its excellent mechanical properties, making it a promising candidate for various applications, particularly in the biomedical field. However, its high susceptibility to corrosion in moist environments, such as body fluids, presents a significant challenge. The rapid reaction with water generates hydrogen gas and forms unstable magnesium oxide layers, severely limiting its application in environments requiring high corrosion resistance. To overcome this limitation, extensive research has focused on developing magnesium alloys reinforced with additional elements and advanced processing techniques. In this study, Mg composites were fabricated using the hot compaction technique. Despite the modifications, the Mg composites demonstrated lower corrosion resistance compared to pure magnesium. The recorded corrosion rates for the composites were 2.06 mm/year and 2.07 mm/year, highlighting the need for further optimization to improve their performance.*

***Keywords*—** *Magnesium composites; Graphene; Yttria; Corrosion behavior.*

I. INTRODUCTION

The demand for advanced metallic biomaterials for artificial implants is steadily increasing, driven by the needs of individuals with bone injuries and degeneration caused by sports-related incidents and accidents, or bone weakness by aging. Biomedical implants are often required to restore functionality of these parts in such cases [1]. In recent years, significant research has been conducted on biodegradable implants, also known as "smart" implants. One key advantage of these implants is their ability to degrade in simulated body fluid (SBF) solutions [2]. Unlike non-degradable implants that may necessitate additional surgical procedures when they become ineffective, biodegradable implants have the ability to completely dissolve after fulfillment of their purpose [3-4]. This avoiding the need for any post implantation surgical intervention to remove the remaining parts of the implanted materials [3, 5]. Consequently, some issues associated with non-degradable implants, such as permanent endothelial dysfunction, long-term physical discomfort, and persistent inflammatory responses, are often reduced or eliminated with biodegradable alternatives [2, 6]. Biodegradable implants offer temporary support during the healing process and have the potential to fully restore some parts of body structure [7-10].

In summary, using biodegradable implants instead of non-degradable implants offers several advantages summarized in the following points [11-13]:

i. Avoiding of Post Implantation Surgical Operations: Biodegradable implants can degrade and dissolve by time, eliminating the need for additional surgical procedures to remove the implant once it has served purpose. This reduces the invasiveness of the treatment and the associated risks and costs.
ii. Reduced Long-Term Complications: Non-degradable implants can sometimes cause long-term complications such as chronic inflammation, discomfort, and adverse tissue reactions. Biodegradable implants, on the other hand, gradually degrade and are absorbed by the body, reducing the likelihood of such complications.
iii. Natural Tissue Reformation: Biodegradable implants enhancing natural tissue reformation and regeneration. As the implant degrades, it provides temporary support to the surrounding tissue, allowing new tissue to grow and replace the implant. This can lead to better functional and aesthetic performance.
iv. Lower Risk of Infection: Biodegradable implants have the advantage of reducing the risk of infection. Non-degradable implants can create a foreign body response, making them susceptible to bacterial infection, growing and colonization. Biodegradable implants, being absorbed by the body, eliminate the presence of a foreign material that could potentially harbor bacteria.
v. Adaptability to Growth and Remodeling: Biodegradable implants can adapt to the growth, remodeling and accelerate tissues regenerations. As the implant degrades, the mechanical load is gradually transferred to the healing tissue, allowing for natural load distribution and remodeling. This can result in improved long-term performance and reduced stress shielding effects on the surrounding tissues.
vi. Avoidance of Implant Removal Surgery: Since biodegradable implants naturally degrade and are absorbed by the body, there is no need for a separate surgery to remove the implant once the healing process is complete. This reduces the overall burden on patients and avoids the associated risks and costs of implant removal.

http://ijses.com/
All rights reserved

Magnesium (Mg), a lightweight and biocompatible metal, has garnered significant attention as a smart material in medical applications due to its unique combination of properties that align well with the demands of advanced biomedical technologies. As a smart material, Mg offers not only excellent strength-to-weight ratios but also a controlled degradation rate that allowing it to gradually dissolve through the human body fluids, minimizing the need for post implantation surgical operations. Its inherent biocompatibility and bioactivity facilitate seamless integration with biological tissues, making it an ideal candidate for applications such as orthopedic implants, stents, and other medical devices where temporary support is needed. Furthermore, ongoing researches deal with Mg functionalization and surface modifications to expand its potential, enabling the development of responsive materials that can adapt to the physiological environment and promote enhanced healing and tissue regeneration [14-15].

Experiments involving the attachment of Mg plates to animal fractured bones have demonstrated promising results. These plates have been found to be sufficiently durable and capable of decomposing as expected after a certain period of time [16]. Similar successful results have been achieved in studies where Mg sheets were implanted in the ends of sheep vertebrae. The sheep skeleton is comparable to the human skeleton, making it a valuable model for these experiments. These studies have shown that the implanted Mg plates not only provide mechanical properties stability but also contribute to accelerated bone formation. This effect leads to the rapid healing of fractures and accelerate the regeneration of bone tissue [17-18]. These findings highlight the potential of Mg-based implants in promoting bone growth and achieving favorable outcomes in fracture healing.

Despite Mg exhibits excellent biocompatibility and biodegradability, it has some disadvantages that limit its widespread use in certain applications. One of the primary drawbacks is its low corrosion resistance, especially when exposed to saltwater or moisture environments, which can lead to rapid degradation [19-20]. Additionally, Mg has relatively poor wear resistance and lower hardness compared to other metals, making it less suitable for applications where surface durability is critical [21]. It is also highly reactive and can be challenging to work with, particularly in processes like welding, where its tendency to melt and burn at relatively low temperatures poses safety risks [22]. Moreover, Mg high thermal expansion and low creep resistance can lead to dimensional instability in high-temperature applications.

In their study, Rashad et al. [23] utilized the SPM (Solid Phase Mixing) approach to synthesize Mg-GNP (Mg-Graphene Nanoplatelets) composites. They observed that; the reinforcement of GNPs in Mg had a significant impact on the mechanical performance of the composite by modifying the structure of the Mg matrix. Similarly, Turan et al. [24-28] investigated the influence of carbon-based additives on the microstructure and properties of Mg-based composites using the SPM approach. This method ensures the uniform dispersion of the additive phase within the Mg alloy matrix, eliminating the need for ball milling. Ball milling is problematic when working with Mg as it generates heat, which can easily lead to ignition of the Mg powder [29]. Consequently, the SPM approach is considered an alternative to ball milling and holds promise for the fabrication of Mg-based composites, which are highly sought after in various engineering applications. GNPs exhibit superior dispersion in different solvents and matrices compared to carbon nano tubes (CNTs). The Mg alloy-GNP composite is produced using a semi-powder metallurgy method combined with the HTE (Hot Torsion Extrusion) procedure, resulting in a uniformly distributed GNP phase within the matrix [28]. Similarly, Sabri et al. [29] synthesized an Mg-based composite with GNPs encapsulated using the SPM approach. Their findings demonstrated that; the homogeneous and even dispersion of a small amounts of GNPs within the Mg-based matrix led to partial agglomeration of GNPs and improved the corrosion and mechanical properties.

This research aims to fabricate and characterize magnesium composites, focusing on their corrosion properties, using the cold-hot compaction technique.

II. Materials, Methods, and Characterization

2.1 Materials

This study utilized a combination of five materials Magnesium (Mg), Tin (Sn), Calcium (Ca), Graphene nanosheets (GNs), and Yttria (Y_2O_3) to develop a magnesium-based nanocomposite.

2.2 Methods

The composite powder mixtures were initially dried and subsequently compacted through cold and hot pressing at a pressure of 800 MPa. They were then transferred to a sintering furnace, where they were processed at a controlled temperature of 450°C for 25 minutes.

2.3 Characterization

The samples are investigated and evaluated by The corrosion resistance of the obtained Mg composite samples was measured by polishing their surfaces using SiC emery paper followed by cleaning with acetone then ethanol. After rinsing the corrosion vessel, it was filled with the freshly prepared simulated saliva fluid (SSF) solution and the corrosion test was conducted at room temperature using an electrochemical workstation (AUTO LAB, PGSTA30, Netherlands). Table 1 list the chemical composition of the prepared simulated saliva fluid (SSF) [30]. The corrosion circuit utilized three electrodes: the working electrode, the reference electrode, and the counter electrode. The working electrode comprised the produced Mg nanocomposite samples. The standard calomel electrode (SCE) with a potential of +0.2444 V was used. The counter electrode is composed of an activated titanium mesh. The electrodes were connected using the Potentiostat model PalSens3, with the reference electrode connected to the white terminal, the counter electrode attached to the red terminal, and the working electrode to the green wire. A steady-state open circuit potential (OCP) was established for one hour. Before starting the experiment, a baseline potential was measured during the OCP phase without applying any ramp potential. The current reading between the working electrode (positive potential) and the counter electrode (negative potential) was approximately 0.01

http://ijses.com/
All rights reserved

μA. The sample was securely placed in a customized corrosion cell and exposed to the environment for 10 minutes. The potential was determined by continuous monitoring when the steady state conditions were reached. Potentiodynamic procedures were selected from the view tab. The exposed surface area of the sample was 0.28 mm². Potentiodynamic polarization was performed by applying a potential starting at -0.3 V and ending at 2.7 V, ±500 mV relative to the evaluated OCP, using a scan rate of 0.001 V/s in steps of 0.002 V. Each specimen for each composition underwent two separate tests.

TABLE 1: Composition of simulated saliva fluid (SSF) [**30**]

Composition	Concentration (g/L)
NaCl	0.4
KCl	0.4
$CaCl_2.2H_2O$	0.795
$NaH_2PO_4.H_2O$	0.690
KSCN	0.30
$Na_2S.9H_2O$	0.005
Urea	1
pH	4

III. Results and Discussion

Electrochemical behavior and corrosion properties

Figure 1 shows potentiodynamic polarization curves of the fabricated Mg nanocomposites in the simulated saliva fluid (SSF) solution. The cathodic polarization curve can be divided into three distinct regions. Region A signifies the passivation stage following the Tafel region. Region B corresponds to the rise in current density as the potential increases. Lastly, region C indicates the occurrence of pitting corrosion. As shown in Figure 1 a difference in the sample behavior in the SSF solution was noted due to varying the type of reinforcement. Through meticulous examination of the Tafel curve, it was revealed that, the corrosion potential of Mg composites shifts towards more positive values in comparison to pure Mg. Likewise, the pitting potential of these composites also shifts towards more positive values when compared with pure Mg. According to the data presented in Table 2, the pure Mg sample demonstrated a potential of -1.66 V and a current density of 4.55E-5 A/cm^2. As a result of alloying Mg with the 15 wt% Sn-5 wt% Ca metallic hybrid, the potential increased to -1.38 V, and the current density rose to 6.43E-5 A/cm^2. The inclusion of GNs in the Mg nanocomposite resulted in a lower potential and current density, indicating a higher level of corrosion resistance. However, the addition of the GNs-Y_2O_3 ceramic hybrid led to the highest current density recorded at 6.47E-5 A/cm^2. As shown in Table 3, the corrosion rate was increased by the addition of both (Sn-Ca) and (GNs-Y_2O_3). The impact of Sn and Ca on Mg alloys' corrosion performance is multifaceted. The addition of Sn and Ca to Mg can deteriorate its corrosion resistance due to several reasons [31-34]. First, Sn and Ca can form secondary phases by interacting with Mg, such as Mg_2Sn or Mg_2Ca, which are electrochemically inert than the Mg matrix. This creates a microgalvanic cell, where the Mg matrix acts as the anode and corrodes preferentially, and accelerating overall corrosion. Second, the addition of Sn and Ca introduces heterogeneity in the microstructure, leading to different electrochemical potentials on the Mg nanocomposite surface, which can promote localized corrosion, such as pitting corrosion. Third, Sn and Ca may segregate at the grain boundaries, weakening these areas' corrosion resistance. Grain boundaries are often preferred sites for corrosion initiation, and the presence of these alloying elements can exacerbate their susceptibility. Furthermore, magnesium typically forms a thin, protective oxide film MgO on its surface that helps slow corrosion. However, adding Sn and Ca can alter the composition and stability of this film, making it less effective in protecting the underlying metal. This altered film may be more porous or less adherent, leading to increased corrosion rates . In Mg-xSn alloys, the precipitation of Mg_2Sn phases aids in passivity promotion but also serves as the site for pitting corrosion initiation [35]. The corrosion in Mg-(2-8wt%) Sn alloys primarily manifests as localized corrosion. Despite the increase in overall dissolution rate with the addition of up to 8 wt% Sn, passivity is enhanced due to the increasing in the H_2 evolution rate and augmented pitting corrosion initiation sites. As per the Mg-Sn binary phase diagram, Sn solid solubility in Mg significantly decreases from 14.85 wt% at the eutectic temperature to 0.45 wt% at 200°C [36]. Hence, Sn addition should be restrained to prevent excessive formation of the Mg_2Sn phase. Calcium is commonly added to AZ series of Mg alloys, and it has been shown to have a beneficial effect on refining the microstructure of these alloys [37, 38]. The corrosion behavior of an AZ61 Mg alloy containing various amounts of Ca has been investigated and reported on previous report. The research findings indicate that as the Ca concentration in the AZ61 alloy was increased, the corrosion rate initially decreased, but then rose sharply. Interestingly, the lowest corrosion rate was observed when the Ca content reached 1%.

The incorporation of Y_2O_3 can result in a more heterogeneous microstructure [39]. This heterogeneity can create localized areas of varying electrochemical activity, promoting localized corrosion. Y_2O_3 can segregate at grain boundaries, which may become sites for preferential corrosion [40]. Grain boundary corrosion can rapidly deteriorate the mechanical properties of the alloy, leading to accelerated the overall corrosion.

The addition of GNs to Mg significantly improves its corrosion resistance by acting as a physical barrier that prevents the penetration of corrosive agents like water and chloride ions [41]. Graphene nano sheets also contribute to refining the microstructure, leading to smaller grain sizes and fewer initiation sites of corrosion. Their high electrical conductivity helps distribute electrochemical potentials more evenly, reducing localized galvanic corrosion [42-44]. Additionally, GNs enhance the formation of a stable, protective oxide layer on the Mg surface, which further protect the metal surface from environmental corrosive media. Together, these effects make Mg more resistant to corrosion when GNs are incorporated. Furthermore, GNs contribute to the formation of a more stable and protective oxide layer on the Mg surface, enhancing passivation and resistance to environmental attack. Lastly, GNs can suppress the anodic dissolution of Mg by either blocking active sites or reducing the anodic reaction rate, thereby lowering the overall corrosion rate.

http://ijses.com/
All rights reserved

IJSES
International Journal of Scientific Engineering and Science
Volume 9, Issue 1, pp. 110-114, 2025. *ISSN (Online): 2456-7361*

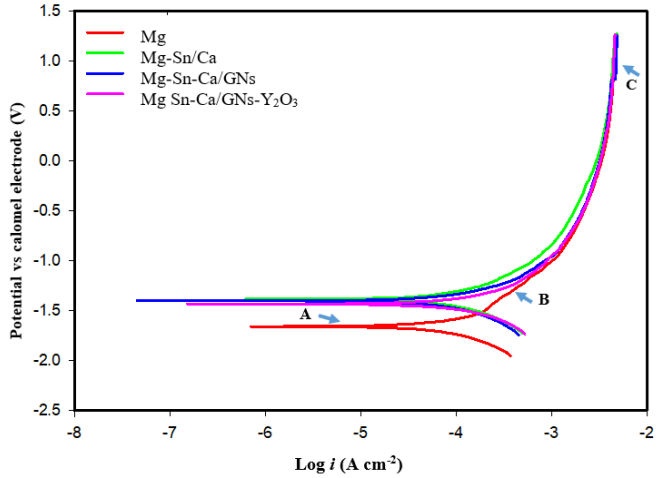

Fig. 1. Potentiodynamic Polarization curves of the fabricated Mg composites in the simulated saliva fluid (SSF) solution.

TABLE: 2. Corrosion parameters and corrosion rate in (mm/year) of the fabricated Mg composites in the simulated saliva fluid (SSF) solution.

Specimen	Ecorr (V)	Jcorr (A/cm^2)	Bc (V/dec)	Ba (V/dec)	Corrosion rate(mm/year)
Mg	**-1.66**	**4.55E-5**	**0.403**	**0.439**	**1.004**
Mg-15 Sn/5 Ca	-1.38	6.43E-5	0.326	0.291	2.06
Mg-15 Sn-5 Ca/1 GNs	-1.40	3.59E-5	0.303	0.255	1.15
Mg-15 Sn-5 Ca/(1 GNs-$1Y_2O_3$)	-1.43	6.47E-5	0.415	0.386	2.07

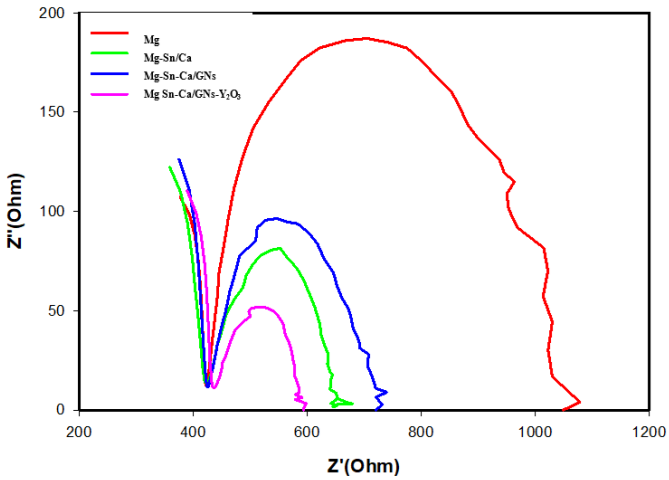

Fig. 2. Nyquist plot of the Mg matrix nanocomposites in the simulated saliva fluid (SSF) solution.

Figure 1 presents the electrochemical impedance spectra of Mg matrix nanocomposites tested at room temperature in the simulated saliva fluid (SSF) solution. The data revealed that, the pure Mg exhibits high impedance. Interestingly, the addition of (Sn-Ca) and (GNs-Y_2O_3) reinforcements to the Mg matrix significantly reduced the impedance values. In contrast, incorporating layered GNs into the Mg matrix resulted in an increase in the impedance. This is attributed to the GNs coating and dispersing along the grain boundaries of the Mg, which enhances the corrosion resistance. The equivalent circuit diagram as shown in Figure 2 was used to fit the electrochemical impedance parameters. Analysis of these parameters revealed that, the pure Mg composite recorded the highest polarization resistance (Rp) value of 660 Ω. Higher Rp values indicate greater corrosion resistance of the material. Reinforcing the Mg with (Sn-Ca) and (GNs-Y_2O_3) reduced the Rp to 234 Ω and 161 Ω, respectively.

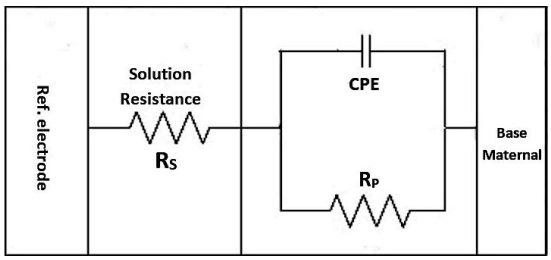

Fig. 3. The equivalent circuit for curve-fitting of the EIS results.

TABLE 3. Parameters obtained by fitting the EIS data to the equivalent circuit.

Specimen	Rp (Ω) Polarization Resistance	Rs(Ω) Solution Resistance	CPE.Y_0(F)
Mg	660	417	1.58E-5
Mg-15 Sn/5 Ca	234	420	2.75E-5
Mg-15 Sn-5 Ca/1 GNs	313	419	2.89E-5
Mg-15 Sn-5 Ca/(1 GNs-$1Y_2O_3$)	161	435	3.75E-5

IV. CONCLUSION

(1) Due to the formation of the Mg_2Sn secondary phase, which is electrochemically innert than the Mg matrix, and the disruption of the MgO layer's stability by the addition of Y_2O_3, making Mg less protective, the Mg-15Sn-5Ca and Mg-15Sn-5Ca/(50%GNs-50%Y_2O_3) composites exhibited the highest corrosion rates, measuring 2.06 mm/year and 2.07 mm/year, respectively.

(2) The Mg exhibited the lowest corrosion rate at 1.004 mm/year, followed by the Mg-Sn-Ca/1% GNs composite at 1.15 mm/year.

REFERENCES

1. Chao-yong ZHAO, Fu-sheng PAN , Hu-cheng PAN, Microstructure, mechanical and bio-corrosion properties of as-extruded Mg–Sn–Ca alloys, Transactions of Nonferrous Metals Society of China, Volume 26, Issue 6, June 2016, Pages 1574-1582
2. Han, H.-S.; Loffredo, S.; Jun, I.; Edwards, J.; Kim, Y.-C.; Seok, H.-K.; Witte, F.; Mantovani, D.; Glyn-Jones, S. Current Status And Outlook On The Clinical Translation Of Biodegradable Metals. Mater. Today 2019, 23, 57–71.
3. Li, N.; Zheng, Y. Novel Magnesium Alloys Developed For Biomedical Application: A Review. J. Mater. Sci. Technol. 2013, 29, 489–502.
4. Zheng, Y.F.; Gu, X.N.; Witte, F. Biodegradable Metals. Mater. Sci. Eng. R. 2014, 77, 1–34.
5. Lee, J.-M.; Salvati, E.A.; Betts, F.; Dicarlo, E.F.; Doty, S.B.; Bullough, P.G. Size Of Metallic And Polyethylene Debris Particles In Failed Cemented Total Hip Replacements. J. Bone Joint. Surg. Br. 1992, 74, 380–384.
6. Bakhsheshi-Rad, H.R.; Akbari, M.; Ismail, A.F.; Aziz, M.; Hadisi, Z.; Pagan, E.; Daroonparvar, M.; Chen, X. Coating Biodegradable Magnesium Alloys With Electrospun Poly-L-Lactic Acid-Åkermanite-Doxycycline Nanofibers For Enhanced Biocompatibility, Antibacterial Activity, And Corrosion Resistance. Surf. Coat. Technol. 2019, 37, 124898.

All rights reserved

7. Hermawan, H. Biodegradable Metals: State Of The Art. In Biodegradable Metals; Springer: Berlin, Germany 2012; Pp. 13–22.
8. Yun, Y.; Dong, Z.; Lee, N.; Liu, Y.; Xue, D.; Guo, X.; Kuhlmann, J.; Doepke, A.; Halsall, H.B.; Heineman, W.; Et Al. Revolutionizing Biodegradable Metals. Mater. Today 2009, 12, 22–32.
9. Moravej, M.; Mantovani, D. Biodegradable Metals For Cardiovascular Stent Application: Interests And New Opportunities. Int. J. Mol. Sci. 2011, 12, 4250–4270.
10. Gong, H.; Agustin, J.; Wootton, D.; Zhou, J.G. Biomimetic Design And Fabrication Of Porous Chitosan–Gelatin Liver Scaffolds With Hierarchical Channel Network. J. Mater. Sci. Mater. Med. 2014, 25, 113–120.
11. Vert, M., Et Al., Terminology For Biorelated Polymers And Applications (Iupac Recommendations 2012), Pure And Applied Chemistry, 84(2), (2012) 377-410.
12. Törmälä, P., Et Al., Biodegradable Implants In Medicine: An Overview, Advanced Materials, 10(18), (1998)1543-1557.
13. Böstman, O., & Pihlajamäki, H., Clinical Biocompatibility Of Biodegradable Orthopaedic Implants For Internal Fixation: A Review, Biomaterials, 21(24), (2000) 2615-2621.
14. Monish P., Hari Krishna K. L., Rajkumar K., Manufacturing And Characterization Of Magnesium Composites Reinforced By Nanoparticles: A Review, Materials Science And Technology, 39:15, (2023), 1858-1876.
15. Amy Chaya Bs., Et Al. Fracture Healing Using Degradable Magnesium Fixation Plates And Screws, Journal Of Oral And Maxillofacial Surgery, 73 (2), (2015), 295-305.
16. Tomic, J.; Wiederstein-Grasser, I.; Schanbacher, M.; Weinberg, A.M. Newly Developed Resorbable Magnesium Biomaterials For Orbital Floor Reconstruction In Caprine And Ovine Animal Models-A Prototype Design And Proof-Of-Principle Study. J. Funct. Biomater. 14, (2023), 339.
17. Gao, H.; Huang, J.; Wei, Q.; He, C. Advances In Animal Models For Studying Bone Fracture Healing. Bioengineering, 10, (2023), 201.
18. Ozgun O., Et Al., Powder Metallurgy Mg-Sn Alloys: Production And Characterization, Transactions B: Mechanical Engineering, 27(3), (2020),1255-1265.
19. Mordike, B. L., & Ebert, T., Magnesium Properties – applications - potential. Materials Science and Engineering: A, 302(1), (2001) 37-45.
20. Gray, J. E., & Luan, B., Protective coatings on magnesium and its alloys - a critical review. Journal of Alloys and Compounds, 336(1-2), (2002) 88-113.
21. Gupta, M., & Sharon, N. M. L. Magnesium, magnesium alloys, and magnesium composites, John Wiley & Sons (2011).
22. Liu, Z., Schaffer, G. B., & Qian, M., Weldability and processing difficulties of magnesium and its alloys, Materials Science Forum, 546-549, (2007) 259-264.
23. Rashad, M.; Pan, F.; Tang, A.; Asif, M.; She, J.; Gou, J.; Mao, J.; Hu, H. Development Of Magnesium-Graphene Nanoplatelets Composite. J Compos. Mater. 2015, 49, 285–293.
24. Turan, M.E.; Sun, Y.; Akgul, Y. Mechanical, Tribological And Corrosion Properties Of Fullerene Reinforced Magnesium Matrix Composites Fabricated By Semi Powder Metallurgy. J. Alloys Compd. 2018, 740, 1149–1158.
25. Turan, M.E.; Zengin, H.; Sun, Y. Dry Sliding Wear Behavior Of (Mwcnt + Gnps) Reinforced Az91 Magnesium Matrix Hybrid Composites. Met. Mater. Int. 2020, 26, 540–550.
26. Turan, M.E.; Sun, Y.; Akgul, Y.; Turen, Y.; Ahlatci, H. The Efect Of Gnps On Wear And Corrosion Behaviors Of Pure Magnesium. J. Alloys Compd. 2017, 724, 14–23.
27. Turan, M.E.; Sun, Y.; Aydin, F.; Zengin, H.; Turen, Y.; Ahlatci, H. Effects Of Carbonaceous Reinforcements On Microstructure And Corrosion Properties Of Magnesium Matrix Composites. Mater. Chem. Phys. 2018, 218, 182–188.
28. Rashad, M.; Pan, F.; Asif, M.; Tang, A. Powder Metallurgy Of Mg–1%Al–1%Sn Alloy Reinforced With Low Content Of Graphene Nanoplatelets (Gnps). J. Ind. Eng. Chem. 2014, 20, 4250–4255.
29. Saberi, A.; Bakhsheshi-Rad, H.R.; Karamian, E.; Kasiri-Asgarani, M.; Ghomi, H. Magnesium-Graphene Nano-Platelet Composites: Corrosion Behavior, Mechanical And Biological Properties. J. Alloys Compd. 2020, 821, 153379.
30. Hossam M. Yehia, Et Al., Effect Of Zirconia Content And Sintering Temperature On The Density, Microstructure, Corrosion, And Biocompatibility Of The Ti–12mo Matrix For Dental Applications, 9 (4), 2020, 8820-8833
31. Gao, L., Zheng, M., Cao, X., Peng, L., & Zhang, D., Effect of Ca and Sn additions on the corrosion behavior of magnesium alloys in NaCl solution, Corrosion Science, 53(4), (2011) 1401-1407.
32. Shi, Z., & Song, G. L., Influence of second phases on the corrosion performance of Mg alloys, Journal of Alloys and Compounds, 390(1-2), (2005) 95-100.
33. Wang, J., Zhang, S., & Liu, M., Effect of Sn addition on the microstructure and corrosion behavior of Mg–Sn–Ca alloys, Materials and Corrosion, 61(10), (2010) 833-839.
34. Song, G., & Atrens, A. Understanding magnesium corrosion—a framework for improved alloy performance, Advanced Engineering Materials, 5(12), (2003) 837-858.
35. Wan X, Tian C, Li Y, Zhou J, Qian S, Su L, Wang L. Effect Of Y2o3 Addition On Microstructure And Properties Of Laser Cladded Al-Si Coatings On Az91d Magnesium Alloy. Materials. 2023; 16(1):338.
36. Heon-Young Ha, et al., Influences of metallurgical factors on the corrosion behavior of extruded binary Mg–Sn alloys, Corrosion Science, 82, May 2014, Pages 369-379.
37. Shanghai Wei, et al., Effects of Sn addition on the microstructure and mechanical properties of as-cast, rolled and annealed Mg–4Zn alloys, Materials Science and Engineering: A, 585, 2013, 139-148.
38. Chen, J.; Li, Q.A.; Zhang, Q.; Zhang, X.Y. The Corrosion Behaviours of AZ61 Magnesium Alloy with the Ca Addition. In Proceedings of the Asia-Pacific Energy Equipment Engineering Research Conference (AP3ER), Zhuhai, China, 13–14 June 2015; pp. 87–90.
39. Yang, Y., & Wang, F. "Effect of Y_2O_3 on the Corrosion Resistance of AZ31 Magnesium Alloy." Journal of Alloys and Compounds, 455(1-2), (2008) 242-247.
40. Chen, J., Yang, J., & Jiang, Y. "Corrosion Behavior of Mg-Y Alloys in Different Aqueous Solutions." Corrosion Science, 53(3), (2011) 794-802.
41. Feng, A., & Han, K., Effect of graphene on corrosion resistance of magnesium alloy in NaCl solution. Journal of Magnesium and Alloys, 4(1), (2016) 60-66.
42. Zeng, R. C., Sun, L., Zheng, Y. F., Cui, H. Z., & Han, E. H., Corrosion and characterization of Mg/graphene oxide composites. Carbon, 66, (2014) 585-590.
43. Liu, P., Liu, Y., & Zhou, H., Improved corrosion resistance of magnesium alloy by graphene oxide coating, Materials Letters, 186, (2017) 288-291.
44. Zhang, X., Shi, Y., Wu, Y., & Han, Y., Graphene oxide as a barrier against corrosion: A review, Journal of Materials Science & Technology, 31(9), (2015) 917-930

http://ijses.com/
All rights reserved